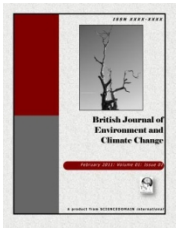

British Journal of Environment & Climate Change
3(1): 44-66, 2013

SCIENCEDOMAIN *international*
www.sciencedomain.org

Assessing Effects of Climate Change on Biogeochemical Cycling of Trace Metals in Alluvial and Coastal Watersheds

Ming-Kuo Lee[1*], Michael Natter[1], Jeff Keevan[1], Kirsten Guerra[1], James Saunders[1], Ashraf Uddin[1], Munir Humayun[2], Yang Wang[2] and Alison R. Keimowitz[3]

[1]Department of Geology and Geography, Auburn University, Auburn, AL, 36839, United States.
[2]Department of Earth, Ocean and Atmospheric Science, Florida State University, Tallahassee, FL 32306, United States.
[3]Department of Chemistry, Vassar College, Poughkeepsie, NY, 12604, United States.

Authors' contributions

This work was carried out in collaboration between all authors. Author MKL managed this project and wrote the first draft of the manuscript. Authors MN, JK, ARK, and YW conducted geological and geochemical analysis of salt marsh samples. Authors KG and MKL conducted the geochemical and hydrologic modeling. Authors JS and AU studied the arsenic distribution in alluvial aquifers. Authors MH, MN and JK conducted LA-ICP-MS analysis of sulfide solids. All authors read and approved the final manuscript.

Research Article

Received 16th January 2013
Accepted 16th March 2013
Published 10th April 2013

ABSTRACT

Assessing the impacts of climate changes on water quality requires an understanding of the biogeochemical cycling of trace metals. Evidence from research on alluvial aquifers and coastal watersheds shows direct impacts of climate change on the fate and transformation of trace metals in natural environments. The case studies presented here use field data and numerical modeling techniques to test assumptions about the effects of climate change on natural arsenic contamination of groundwater in alluvial aquifers and mercury bioaccumulation in coastal salt marshes. The results show that the rises of sea level and river base during the warm Holocene period has led to an overall increase in groundwater arsenic concentration due to the development of reducing geochemical

**Corresponding author: Email: leeming@auburn.edu;*

conditions and sluggish groundwater movement. Modeling results indicate that the intrusion of seawater occurring during high sea-level stand may lead to desorption of arsenic from surface of hydrous oxides due to pH effects and ionic competition for mineral sorbing sites. Our results also show that contamination and bioaccumulation of Hg and other metals in estuarine and coastal ecosystems may be influenced by climate-induced hydrologic modifications (atmospheric deposition, riverine input, salinity level, etc.).

Keywords: Biogeochemical cycle; climate change; sea level rise; trace metals; arsenic; mercury; alluvial aquifers; groundwater; saltwater intrusion; salt marsh; bacterial iron reduction; bacterial sulfate reduction.

1. INTRODUCTION

Trace metals (e.g., mercury, arsenic, lead, cadmium, etc.) are of particular concern in alluvial and coastal watersheds because in excess they are toxic to wildlife and humans [1]. As these elements cycle through natural environments, they undergo biogeochemical reactions that are often coupled to climate change. Many of these toxic heavy metals (e.g., mercury and arsenic) are found at low background concentrations throughout earth's crust [2,3]. These metals may be concentrated locally by natural weathering of bedrocks or anthropogenic activities [4], and their fate and transformation in natural environments often depends on climatic, hydrological and biogeochemical conditions. Climate change can affect every component of the global hydrological cycle, including precipitation, evaporation, groundwater, and runoff [5]. An increase in precipitation, for example, would lead to increases in surface runoff, weathering rates, sediment yields, nutrient loading, and release of heavy metals from both natural and anthropogenic sources.

Various biogeochemical conditions developed in hosting geological environments can naturally cause metals to mobilize, contaminating water resources far from metals' ultimate sources. For example, arsenic released from chemical weathering of source rocks (e.g., black shale's, metamorphic slates, sulfide-rich coals and igneous rocks) would be absorbed by hydrous iron oxides (HFOs) transported by surface streams [6]. Climatic or hydrologic changes may lead to their deposition in stream or coastal environments along with transported organic matter. Subsequently, anaerobic conditions developed in groundwater hosted by these deposits and iron-reducing bacteria could cause the reductive dissolution of As-bearing HFO, releasing arsenic to groundwater [7,8]. Moreover, rising sea level and saltwater intrusion may also lead to substantial desorption of arsenic from hydrous oxides in affected aquifers due to pH effects and ionic competition for HFO sorbing sites [9,10]. Naturally occurring high levels of groundwater arsenic in alluvial aquifers have caused major health problems in many countries [11-14].

Mercury is also of particular concern when methylated because methyl mercury (MeHg) bioaccumulates in organisms and becomes more toxic than inorganic forms. Mercury methylation can be facilitated by sulfate reducing bacteria (SRB) under sulfide-forming (strongly reducing) conditions [15-18] which are themselves promoted by an influx of electron acceptors (i.e., sulfate) and organic carbon [19]. Saltwater intrusion accompanying global sea-level rise provides additional sulfate for bacterial sulfate reduction in coastal sediments. However, sulfide produced by sulfate reduction may also react with dissolved metals to form insoluble metal sulfides; such reaction would decrease the availability of dissolved Hg for methylation by sequestering it in insoluble HgS [18] or Fe-sulfides [14,20-

21]. Fe-sulfides formed in Fe-rich systems also sequester many other dissolved metals (e.g., Cu, Ni, Co, Zn, U, Pb, As, etc.). Moreover, droughts and saltwater intrusion could lead to salinity increase in estuaries and coastal wetlands [22]. Compeau and Bartha [23] showed that bacterial sulfate reduction and Hg methylation may be inhibited in high-salinity environments where sulfate reducing bacteria compete with methanogenic bacteria for limited organic matter produced by fermentation organisms. Climate change and resulting hydrological modification (e.g., droughts, sea level rise) thus could significantly alter the mobility and transformation of Hg and many other metals in aquatic ecosystems.

In this paper, we present case studies on the concentrations, mobility, and transformation of trace metals within alluvial aquifers and coastal watersheds in response to changes in climatic, hydrologic, and biogeochemical conditions. Our main objective is to demonstrate how field data and numerical modeling techniques can be extended and applied to understand the effects of climate change on contaminant fluxes and their transformation in alluvial and coastal environments.

2. CLIMATIC EFFECTS ON LEVEL OF ARSENIC IN AQUIFERS

The first case study examines the link between climate conditions and arsenic level in groundwater of alluvial aquifers over time. During the dry and cold glacial period of Late Pleistocene (120,000-12,000 yr BP), low sea-level stand and greater hydraulic gradients facilitate faster hydrologic flushing of the alluvial aquifers [24,25]. Due to fast hydrologic flushing, groundwater in most Pliocene-Pleistocene alluvial aquifers has very low arsenic contents (Fig. 1). Following the end of the last glacial period, climate warmed up and sea-level gradually and steadily rose during the Holocene (12,000-6,000 yr BP). As a result, fine-grain sediments along with organic matter deposited and filled the river channels. During this warmer Holocene period, high sea level, high river base level, and very gentle hydraulic gradients favor the accumulation and degradation of organic matter, leading to the development of reducing geochemical conditions and sluggish groundwater movement. The reducing conditions triggered the reduction of Fe- and Mn-oxyhydroxides and the release of As, Fe, and Mn into groundwater. The sluggish hydrologic conditions allow little hydrologic flushing and result in an enrichment of arsenic in groundwater in shallow Holocene-age alluvial aquifers (Fig. 1). This sea-level highstand and sluggish hydrologic conditions continued into the civilization and modern day. Multi-century sea-level records reveal a significant acceleration of sea-level rise from the 20th century to the present day [27]. Morhange et al. [28] indicated that the ocean has reached its highest level at present over the last 10,000 years. Thus, slow arsenic flushing in alluvial aquifers will likely continue if this acceleration of sea-level rise remains its current course.

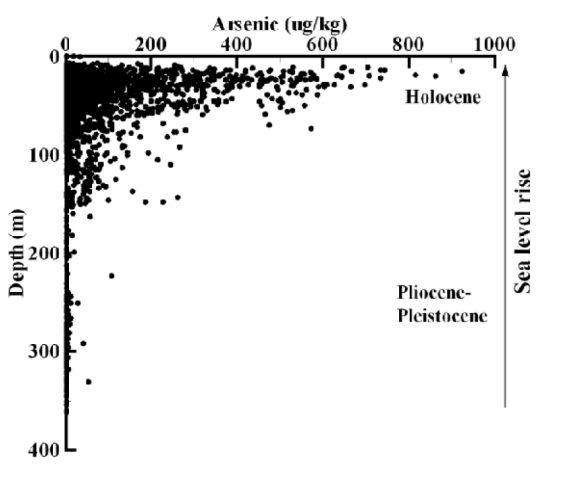

Fig. 1. Diagram shows the depth-wise variations in groundwater arsenic concentration in Pliocene, Pleistocene, and Holocene alluvial aquifers in Bangladesh [26]. Arsenic levels are elevated during Holocene high sea level stand

The widespread arsenic contamination of groundwater in glacial tills worldwide [6] also indicates that arsenic mobilization and enrichment could be enhanced by global warming and glacial melting. Previous workers [29,30] have proposed that the retreat of continental glaciers at the end of the Pleistocene led to rise of sea and river base levels, and deposition of the Holocene alluvium which hosts arsenic derived from glacial erosion of arsenic-bearing bedrocks.

2.1 Hydrologic Flushing in Transport-Dominated Systems (Low Sea Level Stand)

To gain insight into how sea level and hydraulic gradient may control level of groundwater arsenic in alluvial aquifers, we have carried out 1-D simulations of freshwater flushing of an As-contaminated aquifer. The following solute transport equation takes into account the effect of advection, hydrodynamic dispersion, adsorption, and chemical reactions on plume migration:

$$\frac{\partial C_i}{\partial t}(1+\frac{\rho}{\phi}K_d) = D\frac{\partial^2 C_i}{\partial x^2} - v\frac{\partial C_i}{\partial x} + R_i \quad (1)$$

Where C, D, and R_i represent concentration, dispersion coefficient, and chemical reaction rate (by production and consumption) of solute i in a flow system with velocity v. The reaction term R_i for all possible mineral precipitation-dissolution, speciation, redox, and surface complexation reactions [31,32]. Traditional Freundlich and Langmuir sorption theories use distribution coefficients K_d to calculate the ratios of sorbed to dissolved ions. The more comprehensive surface complexation model accounts for electrical charges on the sorbent surface and prescribes mass balance on the sorbing sites.In our model, an alluvial aquifer containing 300 µg/kg of arsenic is infiltrated by dilute rainwater at 25ºC. Assuming a Darcian flow rate of 0.1 m/day, we calculate the distribution of arsenic along the flowpath of 1000 m. To calculate the minimum time required to flush out existing arsenic loads dissolved in groundwater, the reaction term R_i is set to zero (i.e., no arsenic is released from chemical

reactions). The modeling results show that most initial mobile arsenic loads in a considerable part of the aquifer can be flushed out in a few thousand years (Fig. 2). The modeling results are consistent with the ages of As-rich groundwater estimated for Bangladesh Holocene floodplain aquifers [33]. However, longer groundwater residence times (with ^{14}C groundwater ages of 10-40 ka) have been reported in the alluvial plain of Taiwan [34]. It should be noted that the time required to flush the aquifer would be considerably longer for slow flow rates and higher K_d values (not shown), or as long as the geochemical conditions allow continuous arsenic release from solid phases in a reaction-dominated system. The modeling results indicate that climate and related sea level changes could set the stage of regional hydrologic gradients that ultimately control the level and cycling of arsenic in alluvial aquifers.

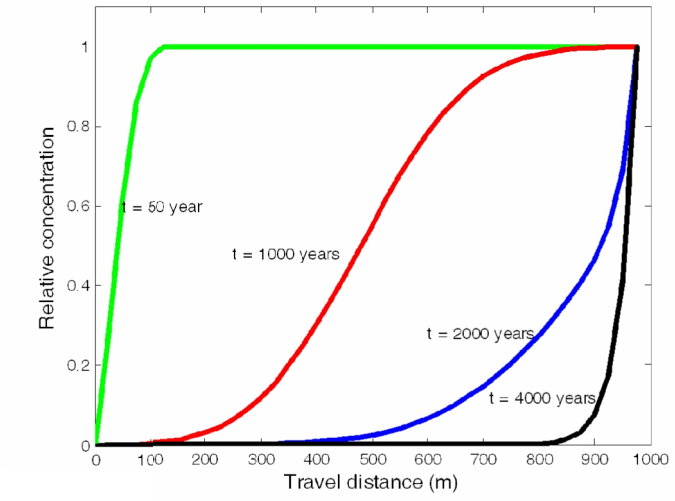

Fig. 2. Calculated breakthrough curves showing the relative concentration of arsenic along a 1000 m-long aquifer in response to infiltration of freshwater after 50, 1000, 2000, and 4000 years. Parameters used in the model: k_d = 5 cm^3/g, α=10 m, ϕ= 0.20, ρ(of sediment) = 2.2 g/cm^3, v = 0.1 m/day. Without new arsenic mobilized from sediments, the initial dissolved arsenic loads will be flushed out in about 4000 years

2.2 Bacterial Reduction of Fe(III) and Mn(IV) Oxides in Reaction-Dominated System (Sea Level High Stand)

High sea level stand and very gentle hydraulic gradients often lead to accumulation of organic matter and the development of reducing (anaerobic) geochemical conditions in river floodplains. We used Geochemist's Workbench (GWB) [35] to trace the sequence of biogeochemical reactions that occur during the bacterial Fe(III) and Mn(IV) oxide reduction, which releases metals and subsequently induces the precipitation of Fe carbonate and sulfide minerals. The program can trace how a fluid's chemistry evolves and which minerals precipitate or dissolve over the course of biogeochemical processes. The purpose of the modeling is to provide insights on the sequence of mineral reactions during the reductive dissolution of Fe and Mn oxides and how mineral reactions affect metal mobility in alluvial aquifers under similar biogeochemical conditions. We begin by equilibrating a typical coastal plain groundwater upstream of an iron reduction zone under aerobic conditions at 25ºC. The calculation uses the water chemical data collected from the Eutaw aquifer of Alabama [36] and assumes that the initial concentrations of Fe and Mn reflect equilibrium with hematite

(Fe_2O_3, a proxy of Fe(III) oxyhydroxides) and pyrolusite (MnO_2, a proxy for Mn(IV) oxyhydroxides) in the sediments. The model then simulates the geochemical effects of titration of organic matter into the system. We consider transformation of pyrolusite and hematite by the following redox reactions:

$$4\ MnO_2\ (\text{pyrolusite}) + CH_3COO^- + 7\ H^+ \rightarrow 4\ Mn^{2+} + 2HCO_3^- + 4H_2O \quad (2)$$

$$4\ Fe_2O_3\ (\text{hematite}) + CH_3COO^- + 15\ H^+ \rightarrow 8\ Fe^{2+} + 2HCO_3^- + 8H_2O \quad (3)$$

In the simulation, fluid reactants containing 500 µmol of acetate (CH_3COO^-) displace existing fluid from the system and the values of Eh slide from +700 mV to -200 mV over the reaction path.

The predicted mineral reactions of manganese and iron oxides (Fig. 3) follow the well-known Ostwald's step rule, which suggests that the solid first formed from a solution would be the least stable polymorph, followed by the more stable phases [37,38]. Pyrolusite in the initial system first becomes thermodynamically unstable during bacterial reduction and transforms over time to a sequence of progressively more stable manganese minerals and species (Fig. 3a) at lower oxidation states:

$$\text{Pyrolusite}(MnO_2) \rightarrow \text{Bixbyite}\ (Mn_2O_3) \rightarrow \text{Rhodochrosite}(MnCO_3)\ \text{or}\ Mn^{2+} \quad (4)$$

Once the reduction of Mn minerals has nearly been completed, the iron redox reactions start (Fig. 3a) and hematite (Fe_2O_3) begins to dissolve to form more stable siderite ($FeCO_3$) or pyrite at low oxidation states. The reduction of Fe(III) oxides occurs under more reducing conditions than Mn minerals. At the later stage of the reaction, reduced metal species also combine with HCO_3^-mineralized from organic sources to form minerals such as rhodochrosite ($MnCO_3$) and siderite ($FeCO_3$). Under highly reducing conditions, aqueous Fe^{2+} reacts with H_2S to form pyrite, which can remove trace elements such as Co, Ni, and As from groundwater by co-precipitation [39,40]. It should be noted that Fe- and Mn-rich groundwaters in many alluvial aquifers are actually saturated with siderite and rhodochrosite [36,41]. Fig. 3b shows the calculated Mn and Fe concentrations in fluid over the same reaction path. It clearly demonstrates how the precipitation and dissolution of various Mn- and Fe- minerals control the mobility of metals in groundwater. Rapid rise and fall of metal concentrations observed over a short distance along the flow path from the recharge zone may be explained by the transformation of various iron and manganese minerals. This modeling result implies that mobilization and re-adsorption (or re-precipitation) of arsenic may occurrapidly over small distances, leading to a dramatic change of As in groundwater from high-As into low-As facies over a very short groundwater flow distance (within meters) [42]. This poses a major challenge to predicting spatio-temporal variations in arsenic concentrations at a local scale. Moreover, the modeling results imply that the transformation of iron and manganese minerals could control mobility of trace metals such as arsenic in alluvial aquifers and requires continued investigation.

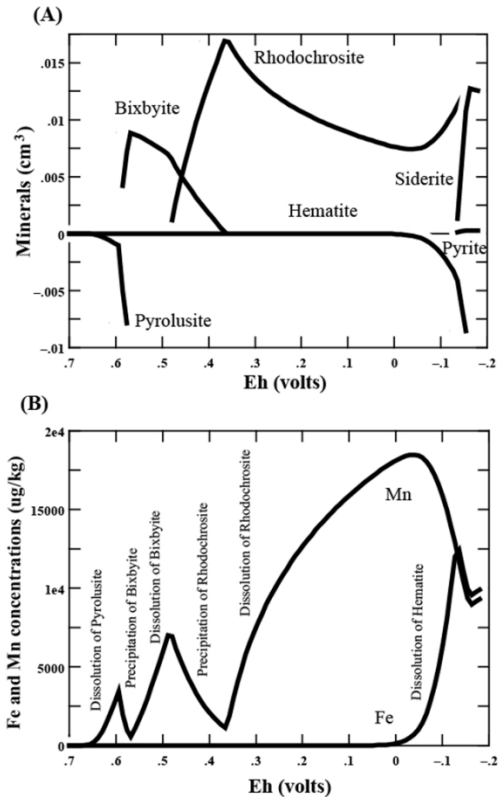

Fig. 3. (A) Predicted sequence of mineralogical reactions resulting from bacteria reduction of Fe and Mn oxides in equilibrium with Moundville groundwater near the Eutaw aquifer outcrop. The plot shows changes in mineral volume as acetate is titrated into the system and Eh decreases with time. Positive changes indicate precipitation, and negative changes show dissolution. (B) Calculated total Mn and Fe concentrations in fluid predicted by the same reaction path model

2.3 Effects of Saltwater Intrusion on Desorption and Mobilization of Arsenic

We use GWB and surface complexation model [31] to simulate the adsorption and desorption of arsenic species associated with oxide minerals in response to sea level rise and saltwater intrusion. The intrusion of seawater in shallow alluvial aquifers may lead to desorption of arsenic from surface of hydrous oxides due to pH effects and ionic competition for HFO sorbing sites. The initial system contains 1 kg of fresh groundwater equilibrated with a small amount (1 g) of $Fe(OH)_3$ at pH 7. The groundwater contains 1 µg/kg of As(III), 1 µg/kg of As(V), and 0.05 molal of NaCl. The calculation prevents the redox coupling between As(III) and As(V). More stable ferric minerals hematite, goethite, and jarosite are suppressed as they are unlikely to reach equilibrium with shallow groundwater at near surface temperatures. Ferric hydroxides used in the simulation have high specific surface areas (600 m^2/g) for sorption reactions. The surface of HFOs is composed of weakly sorbing sites (density = 0.4 mol/mol mineral) and strongly sorbing sites (density = 0.01) [35].

The modeling results show that the initial As sorbed onto $Fe(OH)_3$ is about 19.50 mg/kg (19.22 mg/kg as As(V) and 0.28 mg/kg as As(III)) in equilibrium with a freshwater containing 2 ug/kg of total dissolved As at pH of 7. This result suggests that As is strongly adsorbed by iron oxyhdroxides under aerobic, near-neutral pH conditions. Iron oxide with positive surface charges has a high capability to adsorb negatively-charged anions of arsenic (V) (e.g., $HAsO_4^{2-}$, AsO_4^{3-}). By contrast, As(III), in the form of a non-ionic neutral species $As(OH)_3$, is a poorly sorbing complex. It should be noted that concentrations of arsenic in alluvial and coastal sediments depend on mineralogy (the amounts of Fe oxides and sulfides), texture, and sorbing competition from other ions. For example, the sorbed As contents in Holocene alluvial sediments are in the range of 10-22 mg/kg and 1.2-5.9 mg/kg in parts of the USA [36] and Bangladesh [4], respectively. Seawater pH is in range of 7.5 to 8.5. The simulations assess the desorption of various arsenic species in response to pH increases caused by saltwater intrusion. The modeling results show that significant desorption of As(V) and minor desportion of As(III) occur as pH increases from 7 to 9 in a sliding activity path (Figs. 4a-b). The final arsenic concentration in the fluid increases to more than 250 µg/kg while the As sorbed onto $Fe(OH)_3$ drops to 19.28 mg/kg (19.00 mg/kg of As(V) and 0.28 mg/kg of As(III)). A substantial increase in dissolved as concentrations (> 100 µg/kg) occur when pH > 8.5 (Fig. 4b).

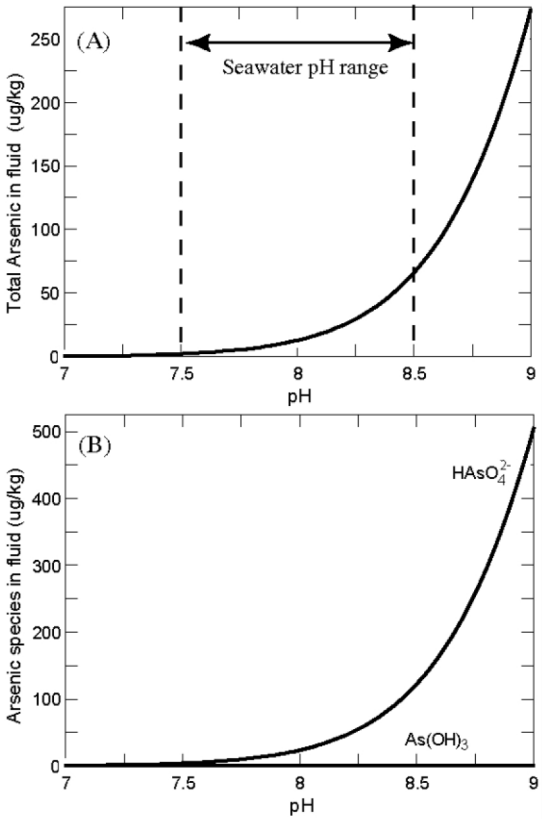

Fig. 4. (A) Dissolved total dissolved arsenic concentrations (B) and the desorption of main As species ($As(OH)_3$ as As(III) and $HAsO_4^{2-}$ as As(V)) versus pH calculated by HFO desorption simulations with pH sliding from 7 to 9

The second geochemical model assesses how various ions in seawater may replace arsenic sorbed onto the surface of HFOs. The modeling results show that the desorption may result in an increase of a few to a few tens of μg As kg^{-1} in solution when the initial system reacts with more than one pore volumes of seawater (Fig. 5). Concurrent increases of arsenic and salinity levels are found in the alluvial aquifers of Taiwan [43] and Bangladesh [26], indicating that many ions (e.g., silicate, carbonate, calcium, sulfate, etc.) in salty groundwater or seawater would compete with arsenic for sorption sites of hydrous oxides. Global warming may cause an additional +0.57 to +1.10 meter of sea level rise by 2100 [44,45]. If the rates of global warming and sea level rise accelerate, more arsenic may be mobilized in aquifers along the coast by ionic competition processes and pH effect.

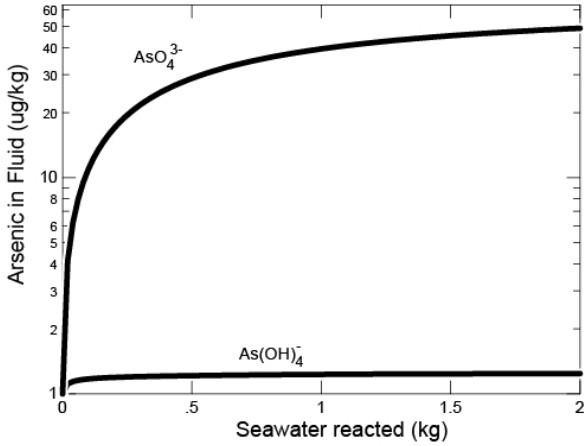

Fig. 5. Calculated dissolved concentrations of arsenic in water as seawater is incrementally added into a freshwater-bearing aquifer, calculated accoring to the Dzombak and Morel (1990) surface complexation model

3. CLIMATIC EFFECTS ON METAL CYCLING IN COASTAL SALT MARSHES

Recent studies suggest that direct atmospheric deposition and riverine input are the primary sources of trace metals (e.g., Hg and As) to estuaries and coastal watersheds [46-49]. Since the brackish water is not potable, metals associated with coastal salt marshes do not pose direct health risks as those in alluvial aquifers. However, in aqueous environments, inorganic mercury is taken up by anaerobic micro-organisms [50] and transformed into the toxic form methyl mercury (CH_3Hg). The health risks associated with biotic accumulation of Hg and other toxic metals underscore the necessity to understand fate and transformation of metals in coastal watersheds. Previous studies have shown that the mixing of large influx of freshwater with seawater in estuarines creates a favorable environment (i.e., the presence of warm, acidic, and low-salinity waters) for mercury methylation [18,23,50-51]. This case study examines the influences of climatic, hydrologic, and microbial processes on biogeochemical cycles of trace metals in coastal watersheds. The Weeks Bay (Fig. 6) in Alabama was chosen because of its close proximity to the mixing zone of freshwater and seawater. The Weeks Bay is impacted by metal pollution like many other estuaries and coastal environments. Largemouth Bass in the Weeks Bay contain mercury concentrations > 1 mg/kg [52,53], the limit set by the Food and Drug Administration. The nearby Wolf Bay (Fig. 6), which has not shown elevated biotic metal concentration, was chosen as a control site for comparison. The main objectives were to (1) analyze total mercury deposition from

atmospheric sources and its seasonal variations, and (2) evaluate sediment geochemical profiles and microbial community to study the source, distribution, and fate of trace metals with depth.

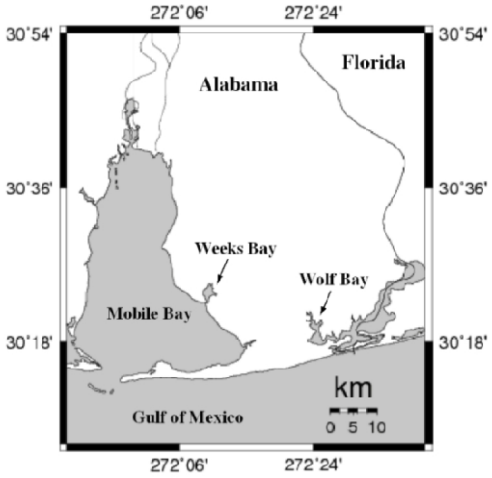

Fig. 6. Simplified location map of the Weeks Bay and Wolf Bay salt marsh study sites in Alabama

3.1 Source of Mercury

Analysis of 2001-2009 data of weekly precipitation and associated mercury levels reveal possible sources of Hg in the Weeks Bay and surrounding areas. The data, obtained from the Mercury Deposition Network (MDN) (http://nadp.sws.uiuc.edu/mdn/), include weekly precipitation (mm), total mercury concentrations (ng/L) in precipitation, and total mercury wet deposition (ng/m^2) collected from two Alabama MDN sites AL02 (Figs. 7 and 8) and AL24 (not shown) near Mobile Bay. Both sites show seasonal trends of highest mercury deposition occurring during wet months of spring, whereas lower mercury deposition generally occurs in the dry summer months (Fig. 7). Clearly higher mercury deposition correlates with periods of higher precipitation (Fig. 8) (correlation coefficients = 0.81 and 0.78 for AL02 and AL24, respectively), supporting the hypothesis that atmospheric deposition represents an important source of mercury and perhaps other airborne metals in the coastal watersheds. Since both Weeks Bay and Wolf Bay receive about the same amount of precipitation, higher levels of Hg and other trace metals found in sediments of the Weeks Bay (see sections below) are likely derived from its higher riverine inputs from Fish River. The Weeks Bay receives far more freshwater inputs from Fish River, the largest surface stream in Baldwin County study area.

The mercury data can be used to assess the impact of climate change on key atmospheric processes that control the transport of mercury from emission to deposition. Atmospheric deposition and riverine input appear to provide the primary pathways by which mercury and other trace metals enter aquatic environments in which bacterial methylation and subsequent accumulation in the food chain can occur. Incremental impacts of climate change on riverine transport and atmospheric deposition of trace metals can be quantified by geochemical analysis of sediments recovered from coastal salt marshes.

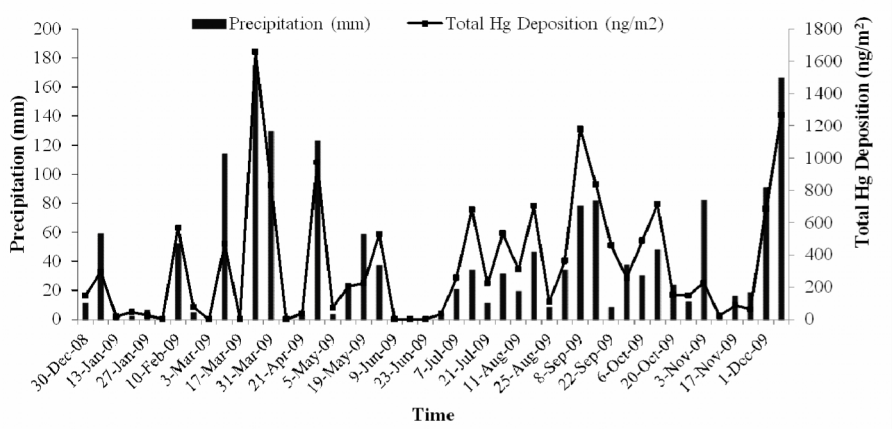

Fig. 7. Fluctuations of total mercury wet deposition (in ng/m^2) responding to rainfall (precipitation, in mm) in southwestern Alabama from December 2008 to December 2009. The diagram shows increased mercury deposition during periods of higher precipitation, suggesting atmospheric deposition of mercury pollution

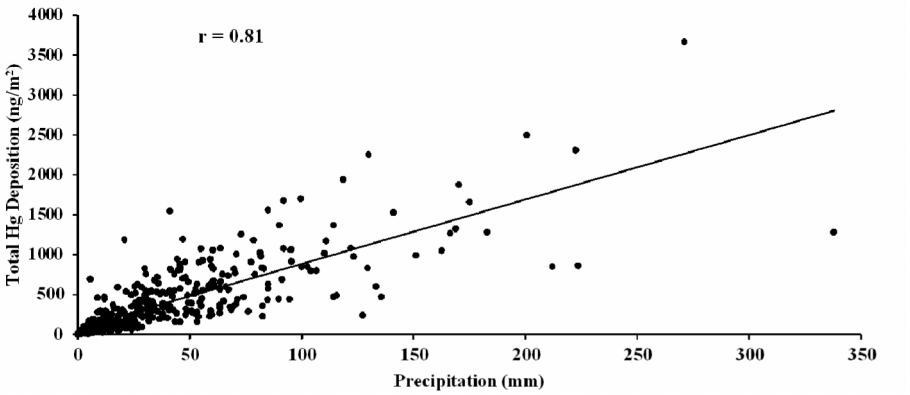

Fig. 8. Bivariate scatter plot with best fit line shows linear (r = 0.81) relationship between total mercury wet deposition (in ng/m^2) and precipitation (mm) collected from the Mercury Deposition Network (MDN). The data were collected from Alabama MDN site AL02 near Mobile Bay from June 2001 to December 2009.

3.2 Sediment Characteristics and Chemistry

Grain size distribution data [54,55] indicate that the Weeks Bay sediments are dominated by fine-grain mud (49 to 53% of clay and 47 to 51% of silt) whereas the Wolf Bay core consists mostly of fine-grain sand (69-85%) with much lower contents of clay and silt. The presence of fine-grain materials is important for retention of metals in the Weeks Bay, as heavy metals tend to concentrate in fine-grain sediments with high-surface sorbing areas.

A total of 20 sediment samples from different depths in the sediment cores have been processed and analyzed for their total organic carbon (TOC) and trace metal contents. The organic carbon contents (TOC) of bulk sediments are higher in the Weeks Bay (2.04±0.24 %) than those in the Wolf Bay (1.76±0.37%). Higher levels of organic carbon in sediments in

the Weeks Bay are likely derived from high rates of erosion and riverine transport of terrestrial carbon associated with Fish River. Organic carbon flux is often higher in watersheds with great weathering and sediment yielding rates [56,57].

Geochemical results from total digestion geochemical analysis of the sediment samples show variations in concentrations of trace elements with depth (Table 1). Enrichment of trace metals and sulfur in salt marsh sediments is revealed by high values aluminum-normalized enrichment factors ANEF(see Appendix).In the Weeks Bay, concentrations of some trace metals (e.g., Cu, Pb, Zn, Fe, Hg, As, etc.) are generally greatest near the water-sediment interface but decline with depth (Fig. 9). The enrichment of trace metals in shallow (post-industrial) sediments is directly related to riverine inputs derived from industrial sources [48]. The Wolf Bay does not show this enrichment pattern. Sedimentation rates in the Gulf coastal marshes are generally less than 0.3 cm/yr [58,59], thus the top 20 cm of sediments (with ages ranging from modern to about 60-70 years) mostly likely exhibit higher levels of trace metals derived from industrial sources. The abundance of fine-grain mud and organic matter in the Weeks Bay further facilitates the retention of trace metals there.

Table 1. Bulk elemental compositions of sediment core recovered from Weeks Bay (WEBSC) and Wolf Bay (WBSC)

Sample ID	Sample Depth(cm)	Ca %	Mg %	Na %	K %	Fe %	Mn mg/kg	Al %	P %	S %
WEBSC	0-3	0.16	0.45	0.79	0.25	3.40	381	2.09	0.043	1.67
WEBSC	3-6	0.18	0.46	0.71	0.24	3.39	384	2.15	0.039	1.85
WEBSC	6-9	0.18	0.53	1.01	0.26	3.27	350	2.17	0.034	1.86
WEBSC	9-12	0.19	0.42	0.78	0.22	2.90	308	1.83	0.030	1.69
WEBSC	12-15	0.20	0.40	0.50	0.20	2.93	314	1.97	0.027	1.86
WEBSC	15-18	0.16	0.41	0.39	0.21	3.12	296	2.19	0.028	1.95
WEBSC	18-21	0.14	0.37	0.28	0.19	2.94	230	1.93	0.024	1.87
WEBSC	21-24	0.13	0.29	0.18	0.15	2.42	167	1.58	0.019	1.48
WEBSC	24-27	0.13	0.34	0.19	0.17	2.57	174	1.60	0.020	1.44
WEBSC	27-30	0.11	0.32	0.17	0.15	2.33	149	1.18	0.016	1.43
WBSC	0-3	0.60	0.10	0.428	0.04	0.25	12	0.31	0.003	0.29
WBSC	3-6	0.05	0.09	0.348	0.04	0.22	7	0.32	0.001	0.25
WBSC	6-9	0.05	0.07	0.247	0.03	0.24	5	0.30	0.002	0.30
WBSC	9-12	0.04	0.07	0.271	0.04	0.28	5	0.34	0.001	0.32
WBSC	12-15	0.04	0.08	0.283	0.04	0.43	6	0.37	0.001	0.51
WBSC	15-18	0.03	0.05	0.196	0.02	0.31	4	0.21	<0.001	0.42
WBSC	18-21	0.04	0.08	0.212	0.04	0.46	8	0.37	0.001	0.59
WBSC	21-24	0.03	0.08	0.220	0.03	0.42	8	0.31	0.001	0.54
WBSC	24-27	0.03	0.06	0.187	0.03	0.43	7	0.25	0.001	0.55
WBSC	27-30	0.05	0.07	0.187	0.03	0.62	8	0.30	0.001	0.69

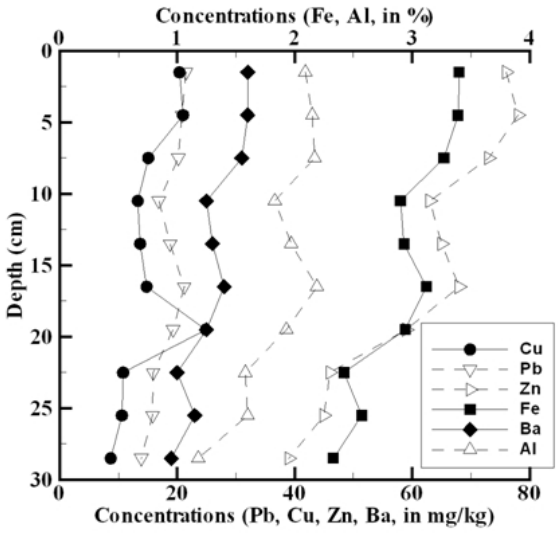

Fig. 9. Depth-wise variations in the concentrations of selected trace metals in sediments of Weeks Bay

The sediment trace metals levels in the Weeks Bay are much higher than those found in the Wolf Bay (Table 2). Sediment mercury concentrations exhibit large depth dependence and range from 0.04 to 0.08 and 0 to 0.02 mg/kg, respectively, at the Weeks Bay and Wolf Bay sites. Levels of As, Pb, Co, Ni, Zn, Cu, Sr, Ba, P, and S in the Weeks Bay sediments are significantly higher than those in the Wolf Bay. Interestingly, concentrations of trace metals are generally low in pore-water extracted from sediments [54]. We hypothesize that high organic matter content and bacterially-mediated sulfate reduction facilitate metal retention via formation of sulfide solids in the marsh sediments.

3.3 Bacterial Sulfate Reduction and Its Impacts on Metal Cycling and Atmosphere CO_2 and O_2

Scanning Electron Microscope (SEM) and laser ablasion inductively coupled plasma mass spectrometry (LA-ICP-MS) analyses reveal the mineralogy, chemical compositions, grain size, and authigenic nature of solids precipitated from pore-water under reducing conditions. Analyzed core samples were chosen from a shallow depth interval (< 20 cm below surface) in the Weeks Bay where metals and sulfur-rich sediments occur. Biogenic sulfide minerals such as pyrite with distinct framboidal form (Fig. 10) are present in the Weeks Bay core samples. The occurrence of aggregates of equi-dimensional spheroids of about 0.5-2 μm (Fig. 10) of iron sulfide has been interpreted as the pyritized corpses of nannobacterial cells embedded in decaying organic matter [60]. The biomineralization of framboidal pyrite was likely performed by sulfate reducing bacteria fueled by organic matter. The formation of framboidal pyrite indicates that sulfate reducing conditions are well established in salt marsh sediments [61,62].

Table 2. Trace metal compositions (in mg/kg) of sediment cores recovered from Week Bay (WEBSC) and Longs Bayou of Wolf Bay (WBSC).

Sample ID	Sample depth (cm)	As	Hg	Cu	Pb	Zn	Co	Ni	V	Cr	La	Ba	Sr	Th
WEBSC	0-3	10.7	0.08	20.4	21.5	76	8.6	13.6	35	32	23	32	33	7.1
WEBSC	3-6	10.5	0.08	21.0	20.8	78	8.4	13.3	35	31	23	32	32	7.2
WEBSC	6-9	10.3	0.08	15.1	20.2	73	8.3	13.1	35	30	23	31	39	7.3
WEBSC	9-12	9.6	0.07	13.3	16.9	63	7.0	11.2	29	26	19	26	33	6.3
WEBSC	12-15	9.8	0.06	13.7	16.8	65	6.8	11.4	34	27	19	26	32	6.7
WEBSC	15-18	10.9	0.07	14.8	21.2	68	7.4	12.7	38	29	20	28	29	7.2
WEBSC	18-21	10.5	0.06	24.9	19.3	59	6.4	11.9	35	27	19	25	27	6.8
WEBSC	21-24	8.3	0.05	10.8	15.9	46	5.2	8.8	29	21	16	20	21	5.7
WEBSC	24-27	9.0	0.05	10.6	15.8	45	6.1	9.9	30	25	18	23	24	6.1
WEBSC	27-30	9.3	0.04	8.7	13.9	39	5.8	8.2	25	19	17	19	22	5.4
WBSC	0-3	1.7	<0.01	3.1	4.4	3	0.5	1.4	10	4	5	4	37	1.7
WBSC	3-6	1.6	<0.01	2.3	4.9	3	0.6	1.3	11	4	5	3	8	1.9
WBSC	6-9	1.9	0.01	1.3	4.4	2	0.6	1.6	11	4	5	3	7	2.1
WBSC	9-12	2.1	<0.01	2.9	4.5	2	0.7	1.2	10	3	5	5	7	2.1
WBSC	12-15	3.2	<0.01	3.5	5.2	2	1.1	1.7	12	5	6	3	8	2.3
WBSC	15-18	1.9	<0.01	3.2	3.5	2	0.6	0.9	8	3	4	2	5	1.5
WBSC	18-21	1.8	0.01	2.7	4.5	3	0.8	1.1	11	7	6	4	8	2.2
WBSC	21-24	1.3	<0.01	2.3	3.9	3	0.7	1.4	8	6	5	4	7	1.8
WBSC	24-27	1.3	<0.01	2.5	3.2	3	0.7	1.4	8	5	4	3	6	1.6
WBSC	27-30	1.8	0.02	3.6	3.9	4	1.2	1.7	10	6	5	4	8	1.8

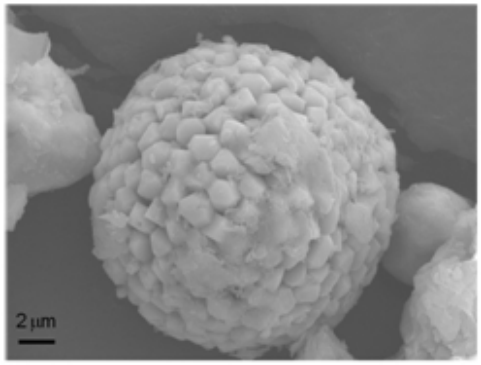

Fig. 10. SEM image of framboidal pyrite formed by sulfate reducing bacteria in Weeks Bay sediments. SEM image shows framboidal texture of pyrite with uniformly sized pyrite microcrystal aggregates

Concentrations of selected trace metals (Table 3) were measured in individual framboid and detrital pyrite grains recovered from the Weeks Bay cores using LA-ICP-MS (Fig. 11). Average S and Fe concentrations in framboid pyrite are 37.9 and 57.4 %, respectively. Mn, Pb, Zn, and V are the most abundant trace elements (average concentrations > 1,000 mg/kg) in the analyzed framboid pyrites. The samples also contain various amounts of Co, Ni, Cu, As, Se, Hg, Mo, and Cd. Hg and Te are present but their concentrations are not calculated due to the lack of standard references. The large variations in chemical composition also suggest a biogenic origin for framboid pyrite. Chemical compositions of detrital pyrite (Table 3) are different from those of framboid pyrite grains. The average trace metal contents are much lower in detrital pyrites than those in the framboid form. Mn, Zn, Ni, and As are the most abundant trace elements in the analyzed detrital pyrites; but their maximum concentrations are less than 65 mg/kg. The early stage framboid iron sulfide in amorphous form is capable of adsorbing and incorporating trace metals into their structure. However over time iron sulfide grains may lose their sorbing capability as they age and re-organize into larger and better-defined atomic structure. Opportunistic microorganisms, such as sulfate reducers, may take advantage of favorable geochemical conditions (i.e., with abundant electron donors/acceptors and available carbon sources) to grow quickly and randomly assemble nearby elements into pyrite with unique framboid form.

Bacterial sulfate reduction may be expressed as one of the following reactions:

$$SO_4^{-2} + CH_2O + H^+ \rightarrow HCO_3^- + H_2S + O_2 \quad (5)$$

$$SO_4^{-2} + 2CH_2O + 2H^+ \rightarrow 2CO_2 + H_2S \quad (6)$$

Where CH_2O represents organic matter. Hydrogen sulfide (H_2S) produced by bacterial sulfate reaction can quickly react with dissolved metals (e.g., Fe^{2+}) in pore-waters to precipitate iron sulfides (Fig. 10):

$$Fe^{2+}(metal) + H_2S(aq) \rightarrow FeS(solid) + 2H^+ \quad (7)$$

Table 3. LA-ICP-MS analyses of selected framboid and detrital pyrite samples from Weeks Bay core

Sample ID	S wt %	Fe wt%	Mn ppm	Pb ppm	Zn ppm	V ppm	Co ppm	Ni ppm	Cu ppm	As ppm	Se ppm	Mo ppm	Cd ppm
Web1	21.6	77.1	8200	2900	940	920	340	9	100	110	30	77	10
Web2	5.2	93.2	9700	3200	1290	950	430	150	160	120	0	72	7
Web3a	15.4	74.1	7900	32	94000	560	620	1770	290	0	0	0	5
Web3b	10.3	76.8	8600	8	118000	610	660	870	26	0	0	0	4
Web4	39.7	55.4	46000	285	1950	360	60	140	89	160	18	13	8
Web5	78.6	20.6	3900	146	1250	2010	45	260	100	66	49	6	18
Web6a*	51.9	48.1	68	17	21	6	9	37	12	62	3	4	0.4
Web6b*	49.9	50.1	64	9	20	5	5	23	7	56	2	11	0.3
Web6c*	52.4	47.5	85	11	28	6	5	21	9	84	3	24	0.5
Web6d*	51.5	48.4	37	11	30	4	5	20	6	61	3	12	0.4
Web7	94.2	4.8	861	1100	340	5700	2	140	77	630	175	400	26

**detrital pyrite grains*

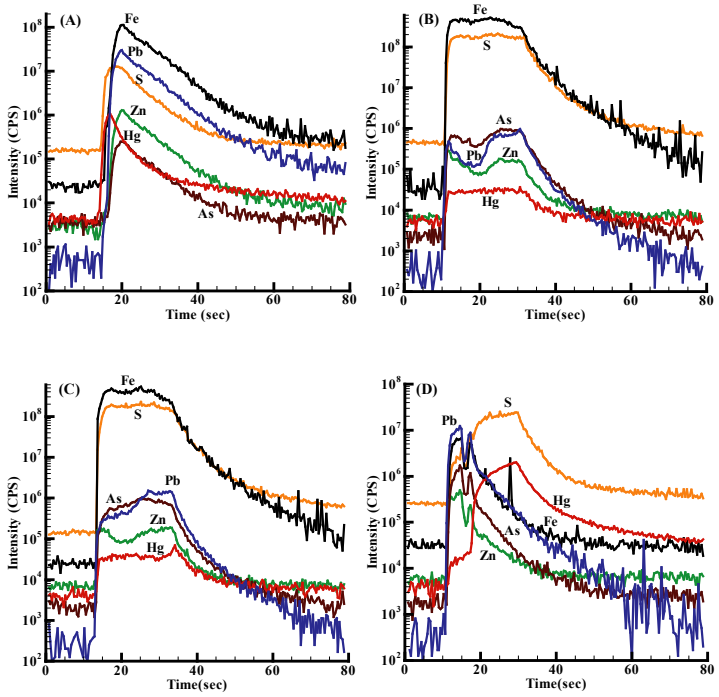

Fig. 11. LA-ICP-MS spectra for weeks bay pyrite samples Web1 (a), Web6a (b), Web6b (c), and Web 7(d). The average trace element concentrations are shown in Table 3. Samples show high levels of Fe and S, along with varying quantities of Pb, Zn, As, Hg, etc. Framboid sample Web 7 shows zoning of several metals (e.g., Fe, Zn, Pb, and As). While trace metal contents show large variations in framboid pyrites, detrital pyrite grains web6a and web6b exhibit "fixed" Fe/S molar ratios ranging from 0.52-0.58

Reaction (7) not only limits the mobility of trace metals and their dissolved loads in pore-water, it may also regulate CO_2 and O_2 oxygen levels in the atmosphere. The roles of sulfur cycling in regulating atmospheric carbon and oxygen have often been ignored. This study shows that pyrite-like sulfide forms in salt marshes (Fig. 10) or sea floor [20] when microbes take up sulfur in the form of sulfate (with four bound oxygen atoms) in seawater and consequently release sulfide along with extra oxygen as free O_2 or CO_2. More research is needed to assess how bacterial sulfate reduction and sulfide formation may regulate global oxygen and carbon cycles under current changing climate conditions and rising sea levels.

Elucidating the bacterial sulfate reduction can help understand the climatic and hydrological factors controlling the contamination and bioaccumulation of Hg and other metals in aquatic ecosystems. Sulfide produced from sulfate reduction may also react with dissolved metals to form insoluble metal sulfides (Fig. 10); such reaction would decrease the availability of dissolved Hg for methylation by sequestering it in insoluble metal sulfides [18,20-21]. Moreover, Compeau and Bartha [23] showed that Hg methylation may be inhibited in high-salinity environments where sulfate reducing bacteria compete with methanogenic bacteria for limited organic matter produced by fermentation organisms. Sea level rise has resulted in salinity increases of many coastal estuaries and bays and intrusion of seawater into fresh coastal ground water resources [63]. Climate change models have predicted that the global

sea level could increase between 18 cm and 59 cm during this century [64]; other worst-case scenario predictions have forecasted even higher sea-level rise of up to 180 cm in part of the Gulf of Mexico Coast regions [65]. We argue that climate change and related hydrological modification will significantly impact the biogeochemical cycles of heavy metals and carbon in the coastal aquatic ecosystems.

3. FUTURE CHALLENGES

One of the most noteworthy predicted biogeochemical changes in response to climate change and sea-level rise is a widespread increase in groundwater arsenic levels in alluvial and coastal watersheds. Our field data and computer models link the enrichment of groundwater arsenic with high sea-level stand, high river base level, sluggish hydrologic flushing, and reducing geochemical conditions. The biogeochemical cycling of trace metals in alluvial and coastal environments is very complex because it has to be considered within the context of geology (e.g., grain size and mineralogy) and many climatic, hydrologic, and microbial proccesses, such as changes in temperature, salinity, pH, and redox conditions, bacterial-mediated biogeochemical reactions (i.e., iron and sulfate reduction, methylation), biomineralization (e.g., formation of iron sulfide), and adsorption/desorption reactions. Hydrologic and geochemical models are particularly useful for providing insights into these complex interactions but are limited to represent processes to the extent that they are quantitatively formulated. Some of the modeling results may be better constrained by field data when available. Measuring climate events, hydrological modifications, and biogeochemical processes in the field over time could be challenging because they may occur at different temporal and spatial scales in different geological environments. Perhaps the greatest challenge is in our understanding of the feedback loops between the climate system and biogeochemical cycling. For example, climate-induced biogeochemical processes may provide a source or a sink for oxygen or greenhouse gases in the atmosphere. An integrated research framework consisting of numerical modeling, long-term monitoring, laboratory experiments will be necessary for building a comprehensive understanding of the complex response of biogeochemical cycling of trace metals to climate change.

ACKNOWLEDGEMENTS

This research was partly supported by grants from the National Science Foundation (NSF-0445259 and NSF-1048925). We thank Dr. Scott Phipps and Michael Shelton (Weeks Bay Reserve) for field assistance and helpful discussions concerning Weeks Bay geology and hydrological system. Auburn geology graduate students Mohammad Shamsudduha, Mohammad Huq, Jamey Turner, Robert Monrreal, Lee Beasley, and Brian Woodall were involved in field sampling and laboratory analysis of sediment and groundwater samples. Thanks are also due to Dr. Bart Prorok and Dr. Charles Savrda for their assistant in SEM-EDAX and total carbon analysis at Auburn University.

COMPETING INTERESTS

Authors have declared that no competing interests exist.

REFERENCES

1. Cohen T, Que Hee SS, Ambrose RF. Trace metals in Fish and Invertebrates of thee California Coastal Wetlands. Marine Pollution Bulletin. 2001;42:224-232.
2. Wedepohl KH. The composition of the continental crust. Geochimica et Cosmochimica Acta. 1995;59:1217-1232.
3. Drever JI. The Geochemistry of Natural Water. 3rd ed. Upper Saddle River, New Jersey: Prentice Hall; 1997.
4. 4. Smedley PL, Kinniburgh DG. A review of the source, behavior and distribution of arsenic in natural waters. Applied Geochemistry. 2002;17:517-568.
5. Chang H, Jung I-W. Spatial and temporal changes in runoff caused by climate change in a complex large river basin in Oregon. Journal of Hydrology. 2010;388:186-207.
6. Saunders JA, Lee M-K, Uddin A, Mohammad S, Wilkin R, Fayek M, Korte N. Natural arsenic contamination of Holocene alluvial aquifers by linked glaciation, weathering, and microbial processes. Geochemistry, Geophysics, and Geosystems. 2005;6(4):Q04006, doi:10.1029/2004GC000803.
7. Nickson R, McArthur J, Burgess W, Ahmed KM, Ravenscroft P, Rahman M. Arsenic poisoning of Bangladesh groundwater. Nature, 1998;395:338.
8. Islam F, Gault A, Boothman C, Polya D, Charnock J, Chatterjee D, Lloyd J. Role of metal-reducing bacteria in arsenic release from Bengal delta sediments. Nature. 2004;430:68-71.
9. Impellitteri CA. Effects of pH and phosphate on metal distribution with emphasis on As speciation and mobilization in soils from a lead smelting site. Science of Total Environment. 2005;345:175-190.
10. Tyrovola K, Nikolaidis NP. Arsenic mobility and stabilization in topsoils. Water Research, 2009;43:1589-1596.
11. Nickson RT, McArthur JM, Ravenscroft P, Burgess WG, Ahmed KM. Mechanism of arsenic release to groundwater, Bangladesh and West Bengal. Applied Geochemistry. 2000;15:403-413.
12. Smith AH, Lingas EO, Radman M. Contamination of drinking-water by arsenic in Bangladesh: A public health emergency. Bulletin of the World Health Organization. 2000;78:1093-1103.
13. Harvey CF, Swartz CH, Badruzzman B, Keon NE, Yu W, Ali A, Jay J, Beckie R, Niedan V, Brabander D, Oates P, Ashfaque K, Islam S, Hemond HF, Ahmed F. Arsenic mobility and groundwater extraction in Bangladesh. Science. 2002;298:1602-1606.
14. Saunders JA, Lee M-K, Shamsudduha M, Dhakal P, Uddin A, Chowdury MT, Ahmed KM. Geochemistry and mineralogy of arsenic in (natural) anaerobic groundwaters. Applied Geochemistry. 2008;23:3205-3214.
15. Compeau G, Bartha R. Methylation and demethylation of mercury under controlled redox, pH, and salinity conditions. Applied Environmental Microbiology. 1984;48:1203-1207.
16. King JK, Harmon SM, Fu TT, Gladden JB. Mercury removal, methylmercury formation, and sulfate-reducing bacteria in wetland mesocosms, Chemosphere. 2002;46:859-870.
17. DeLaune RD, Jugsujinda A, Devai I, Patrick WH Jr. Relationship of sediment redox conditions to methylmercury in surface sediment of Louisiana Lakes. Journal of Environmental Science and Health. 2004;39:1925-1935.
18. Kongchum MI, Devai RD, Delaune A, Jugsujinda D. Total mercury and methylmercury in freshwater and salt marsh soils of the Mississippi river deltaic plain. Chemosphere. 2006;63:1300-1303.

19. Sunderland EM, Gobas FA, Heyes A, Branfireun BA, Bayer AK, Cranston RE, Parsons MB. Speciation and bioavailability of mercury in well-mixed estuarine sediments. Marine Chemistry. 2004;90:91-105.
20. Huerta-Diaz MA, Morse JW. Pyritization of trace metals in anoxic marine sediments. Geochimica et Cosmochimica Acta. 1992;56:2681-2702.
21. Lee M-K, Saunders JA. Effects of pH on metals precipitation and sorption: Field bioremediation and geochemical modeling approaches. Vadose Zone Journal. 2003;2:177-185.
22. Sklar FH, Browder JA. Coastal environmental impacts brought about by alterations to freshwater flow in the Gulf of Mexico. Environmental Management. 1998;22:547-562.
23. Compeau G, Bartha R. Effect of salinity on mercury methylating activity of sulfate-reducing bacteria in estuarine sediments. Applied Environmental Microbiology. 1987;53:261-265.
24. Ravenscroft P, Burgess WG, Ahmed KM, Burren M, Perrin J. Arsenic in groundwater of the Bengal basin, Bangladesh: Distribution, field relations, and hydrogeological setting. Hydrogeology Journal. 2004;10.1007/s10040-003-0314-0.
25. Shamsudduha M, Marzen LJ, Uddin A, Lee M-K, Saunders JA. Groundwater arsenic-contamination in Bangladesh: control of surface elevation, slope, and groundwater gradient on spatial arsenic distribution. Environmental Geology. 2008;57:1521-1535.
26. BGS and DPHE. Arsenic Contamination of Groundwater in Bangladesh, v. 2, Final Report, BGS Technical Report WC/00/19; 2001.
27. Church JA, White NJ. A 20th century acceleration in global sea-level rise. Geophysical Research Letters. 2006;33:L01602, doi:10.1029/2005GL024826.
28. Morhange C, Laborel J, Hesnard A. Changes of relative sea level during the past 5000 years in the ancient harbor of Marseilles, Southern France. Palaeogeography, Palaeoclimatology, Palaeoecology. 2001;166:319-329.
29. Acharyya SK, Lahiri S, Raymahashay BC, Bhowmik A. Arsenic toxicity of groundwater in parts of the Bengal Basin in India and Bangladesh; the role of Quaternary stratigraphy and Holocene sea-level fluctuation. Environmental Geology. 2000;39:1127-1137.
30. McArthur JM, Ravenscroft P, Safiulla S, Thirlwall MF. Arsenic in groundwater: testing pollution mechanisms for sedimentary aquifers in Bangladesh. Water Resources Research. 2001;37:109-11.
31. Dzombak DA, Morel FMM. Surface Complexation Modeling: Hydrous Ferric Oxide. New York: John Wiley & Son; 1990.
32. Stumm W. Chemistry of the Solid-Water Interface. New-York: Wiley; 1992.
33. van Geen A, Zheng Y, Goodbred S Jr, Horneman A. Aziz Z, Cheng Z, Stute M, Mailloux B, Weinman B, Hoque MA, Seddique AA, Hossain MS, Chowdhury SH, Ahmed KM. Flushing history as a hydrogeological control on the regional distribution of arsenic in shallow groundwater of the Bengal Basin. Environmental Science and Technology. 2008;42:2283-2288.
34. Chen K-Y, Liu T-K. Major factors controlling arsenic occurrence in the groundwater and sediments of Chianan coastal plain, SW Taiwan. Terrestrial, Atmospheric, & Oceanic Sciences. 2007;18:975-994.
35. Bethke CM Geochemical and Biogeochemical Reaction Modeling. 2nd ed. Cambridge: Cambridge University Press; 2008.
36. Penny E, Lee M-K, Morton C. Groundwater and microbial processes of the Alabama coastal plain aquifers. Water Resources Research. 2003;39(11):1320, doi:10.1029/2003WR001963.
37. Morse JW, Casey WH. Ostwald processes and mineral paragenesis in sediments. American Journal of Science. 1988;288:537-560.

38. Norden SH, Sibley D. Dolomite stoichiometry and Ostwald's step rule. Geochimica et Cosmochimica Acta. 1994;58:191-196.
39. Saunders JA, Prichett MA, Cook RB. Geochemistry of biogenic pyrite and ferromanganese stream coatings: A bacteria connection? Geomicrobiology Journal. 1997;14:203-217.
40. Lehner SW, Savage KS, Ayers JC. Vapor growth and characterization of pyrite (FeS2) doped with Co, Ni, and As: Variations in semiconducting properties. Journal of Crystal Growth. 2006;286:306-317.
41. Lee M-K, Griffin J, Saunders JA, Wang Y, Jean J. Reactive transport of trace elements and isotopes in Alabama coastal plain aquifers. Journal of Geophysical Research. 2007;112:G02026, doi:10.1029/2006JG000238.
42. Yu WH, Harvey CM, Harvey CF. Arsenic in groundwater in Bangladesh: A geostatistical and epidemiological framework for evaluating health effects and potential remedies. Water Resources Research. 2003;39:1146, doi:10.1029/2002WR001327.
43. Nath B, Jean J, Lee M-K, Liu C-C. Geochemistry of high arsenic groundwater in Chia-Nan plain, Southwestern Taiwan: Possible sources and reactive transport of arsenic. Journal of Contaminant Hydrology. 2008;99:85-96.
44. Meier MF, Dyurgerov MB, Rick UK, O'Neel S, Pfeffer WT, Robert S, Anderson RS, Suzanne P, Anderson SP, Glazovsky AF. Glaciers dominate eustatic sea-level rise in the 21st Century. Science. 2007;317:1064-1067.
45. Jevrejeva S, Moore JC, Grinsted A. Sea level projections to AD2500 with a new generation of climate change scenarios. Global and Planetary Change. 2012;80:14-20.
46. Mason RP, Fitzgerald WF, Morel FMM. Biogeochemical cycling of elemental mercury: Anthropogenic influences. Geochimica et Cosmochimica Acta. 1994;58: 3191-3198.
47. Mason RP, Lawson NM, Lawrence AL, Leaner JJ, Lee JG, Sheu G. Mercury in the Chesapeake Bay. Marine Chemistry. 1999;65:77-96.
48. Bonzongo JC, Lyons WB. Impact of land use and physiochemical settings on aqueous methylmercury levels in the Mobile-Alabama River System. Ambio, 2004;33:328-333.
49. Engle MA, Tate MT, Krabbenhoft DP, Schauer JJ, Kolker A, Shanley JB, Bothner MH. Comparison of atmospheric mercury speciation and deposition at noe sites across central and eastern North America. Journal of Geophysical Research, 2010;115:D18306, doi:10.1029/2010JD014064.
50. Ullrich SM, Tanton TW, Abdrashitova SA. Mercury in the aquatic environment: A review of factors affecting methylation. Critical Review Environmental Science and Technology. 2001;31:241-293.
51. Celo VD, Lean RS, Scott SL. Abiotic methylation of mercury in the aquatic environment. Science of Total Environment. 2006;368:126-137.
52. ADEM. The ADEM Fish Tissue Monitoring Program 1991-1995: Alabama Department of Environmental Management; 1996.
53. ADPH. Alabama Department of Public Health issues 2008 fish consumption advisories: Alabama Department of Public Health; 2008.
54. Natter M. Fate and transformation of oils and trace metals in Alabama and Louisiana coastal marsh sediments associated with the British Petroleum Gulf oil spill. Master Thesis, Auburn University, Auburn, Alabama; 2012.
55. Natter M, Keevan J, Keimowitz AR, Okeke B, Wang Y, Son A, Lee M-K. Level and degradation of Deepwater Horizon spilled oil in coastal marsh sediments and pore-water. Environmental Science and Technology. 2012;46:5744-5755.
56. Lyons BW, Nezat CA, Carey AE, Hicks DM. Organic carbon fluxes to the ocean from high-standing islands. Geology. 2002;30:443-446.

57. Carey AE, Kao S-J, Hicks DM, Nezat CA, Lyons WB.The geochemistry of rivers in tectonically active areas of Taiwan and New Zealand. In: Sean D, Willett SD, Hovius N, Brandon MT, Fisher DM, editors. Tectonics, Climate, and Landscape Evolution. Geological Society of American Special Paper. 2006;398:339-351.
58. Callaway JC, DeLaune RD, Patrick WH Jr. Sediment accretion rates from four coastal wetlands along the Gulf of Mexico. Journal of Coastal Research. 1997;13:181-191.
59. Mertz LM, Hart M, Jaeger J. Use of radioisotopes to constrain preservation potential of paleostorm deposits in Gulf of Mexico coastal sediments. Abstracts with Programs. Geological Society of America. 2003;35(1):14.
60. Folk RL. Nannobacteria and the formation of framboidal pyrite: Textual evidence. Journal of Earth System Science. 2005;114:369-374.
61. Wilkin RT, Barnes HL, Brantley SL. The size distribution of framboidal pyrite in modern sediments: An indicator of redox conditions. Geochimica et Cosmochimica Acta. 1996;60:3897-3912.
62. Wilkin RT, Barnes HL. Formation processes of frambiodal pyrite. Geochimica et Cosmochimica Acta. 1997;61:323-339.
63. USGS. Ground Water Atlas of the United States, Alabama, Florida, Georgia, South Carolina, HA 730-G. Accessed 2 April 2013. Available: http://pubs.usgs.gov/ha/ha730/ch_g/G-text4.html
64. IPCC. Climate Change 2007: Impacts, Adaptation and Vulnerability, Contribution of Working Group II to the Fourth Assessment Report of the Intergovernmental Panel on Climate Change. In: Parry ML, Canziani OF, Palutikof JP, van der Linden PJ, Hanson CE, editors. Cambridge, UK: Cambridge University Press; 2007.
65. Vermeer M, Rahmstorf S. Global sea level linked to global temperature. Proceeding National Academy of Science. 2009;106(51):21527-21532.

APPENDIX

Enrichment of sulfur and chalcophile ("sulfur-loving") elements in salt marsh sediments is revealed by the aluminum-normalized enrichment factor (ANEF):

$$\frac{Me_{sample} / Al_{sample}}{Me_{crust} / Al_{crust}} \quad \text{(A1)}$$

Here *Me* represent trace metals in sediments and *Al* (aluminum) is the selected reference metal in crust. Crustal concentrations of various elements were calculated by Wedepohl [2]. ANEF factors to a large degree filter out the inputs from terrigenous sediment sources. Since there are no known anthropogenic sources of aluminum to sediments, any metals with substantial post-industrial inputs would have positive ANEF anomalies. ANEF may also provide useful insights on reactivity relationship such as the retention of chalcophile metals in sediments via bacterial sulfate reduction and formation of sulfide solids. Our calculations (Supplementary Fig. A1) indicate that Weeks Bay sediments have high ANEF values for S (75.5±9.0) and As (21.0±3.5). Other trace elements such as Cu, Pb, Zn, Fe, and Hg also display relatively high ANEF values (>4). Sediments in Wolf Bay exhibit similarly high ANEF values in S (120.9±45.8), As (23.5±6.3), and certain trace elements, although their absolute concentrations are lower with respect to those of Weeks Bay (Tables 1 and 2).

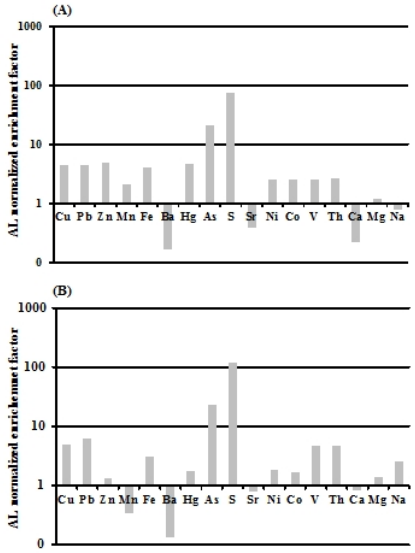

Fig. A1. Calculated average aluminum-normalized enrichment factors of various elements in (A) Weeks Bay and (B) Wolf Bay sediments.

Peer-review history:
The peer review history for this paper can be accessed here:
http://www.sciencedomain.org/review-history.php?iid=218&id=10&aid=1219